ELSEVIER

Available online at www.sciencedirect.com
SCIENCE DIRECT®

Renewable Energy xx (xxxx) 1–20

RENEWABLE ENERGY

www.elsevier.com/locate/renene

Novel ocean energy permanent magnet linear generator buoy

K. Rhinefrank[a], E.B. Agamloh[a], A. von Jouanne[a,*], A.K. Wallace[a], J. Prudell[a], K. Kimble[a], J. Aills[a], E. Schmidt[a], P. Chan[b], B. Sweeny[b], A. Schacher[a]

[a]*School of Electrical Engineering and Computer Science, Oregon State University, Corvallis, OR 97331-3211, USA*
[b]*Department of Mechanical Engineering, Oregon State University, Corvallis, OR 97331-3211, USA*

Received 12 May 2005; accepted 27 July 2005

Abstract

This paper describes the research, design, construction and prototype testing process of a novel ocean energy direct drive permanent magnet linear generator buoy. The buoy employs the vertical component of the motion of ocean waves to power a linear generator. The generator consists of a permanent magnet field system (mounted on the central translator shaft) and an armature, in which the power is generated (mounted on the buoy). The translator shaft is anchored to the sea floor, and the buoy/floater moves armature coils relative to the permanent magnet translator to induce voltages. The electrical and mechanical structures of the buoy generator are provided, along with performance characteristics, including voltage, current and developed power.
© 2005 Published by Elsevier Ltd.

Keywords: Linear generator; Buoy; Ocean wave energy

1. Introduction

The solutions to today's energy challenges need to be found through increased electricity generation using alternative, renewable and clean energy sources. An

* Corresponding author. Tel.: +1 541 737 0831; fax: +1 541 737 1300.
E-mail address: avj@eecs.oregonstate.edu (A. von Jouanne).

0960-1481/$ - see front matter © 2005 Published by Elsevier Ltd.
doi:10.1016/j.renene.2005.07.005

UNCORRECTED PROOF

Nomenclature

D	buoy diameter
b	hydrodynamic damping
m_v	buoy virtual mass
c	spring constant
a	buoy added mass
F	wave exciting force
L	inductance
λ	flux linkage
f	power take off thrust
N	number of turns in phase
v	phase voltage
i	phase current
r	phase resistance
E	electromotive force
z	vertical displacement of the translator relative to the stator
τ	pole pitch of the generator
$\hat{\phi}$	peak flux
$\bar{A}$	ratio of wave amplitude and amplitude of motion
ϕ	is the phase angle between the voltage and current

extremely promising source of energy exists in the world's oceans. It is estimated that if 0.2% of the ocean's untapped energy could be harnessed, it could provide power sufficient for the entire world [1]. The co-authors are part of a strategic, multidisciplinary ocean energy team comprised of graduate and undergraduate students investigating novel ocean wave energy extraction approaches. The ocean energy team's research and development goals are driven by the important issues of survivability, reliability and maintainability, in addition to efficient and high quality power take-off systems.

2. Wave energy extraction technologies

The world's first wave energy device patent was registered in 1799 by Girard, in Paris. After more than 200 years' development, there are currently more than 1500 wave energy device patents. Historically, there have been two booms of interest in the research of wave energy, corresponding to the 1970 s oil crisis and pollution concerns as well as concerns regarding natural resource reserves since the mid 1990 s. Depending on the distance between the conversion devices and the shoreline, wave energy systems can be classified as shoreline, nearshore and offshore extraction systems.

UNCORRECTED PROOF

2.1. Shoreline devices

Shoreline devices are devices fixed to or embedded in the shoreline. Examples include the oscillating water column (OWC), which is the most developed of the shoreline devices. An OWC system has a partially submerged hollow air chamber, which opens to the sea under the water line. A wave enters the air chamber and forces the air in the column to pass through a turbine; when the wave retreats, the air will be drawn back and pass through the turbine again (Fig. 1, [2]). The turbine can be unidirectional or self-rectified. The unidirectional 'Wells turbine' is the best-known turbine for this kind of application. The world's first commercial wave power unit is the LIMPET 500, an OWC system mounted on the cliffs of the Islay island in Scotland by Wavegen. It generates a peak power of 500 kW, enough to provide service for about 400 island homes. This system has successfully fed electricity into the UK's national grid since November 2000.

Another representative of OWC technology is in development by Energetech in Australia [3]. Compared to the LIMPET, it uses a variable pitch turbine instead of the Wells to achieve higher system efficiency, and it has a relatively cheap parabolic wall behind the OWC to focus the wave energy on to the more expensive collector and associated plant.

The 'pendulum' was developed by the Japan Marine Science and Technology Center (JAMSTEC). It consists of a concrete box with one end open to the sea. A steel pendulum flap is hinged over this opening. Waves cause the pendulum flap to swing back and forth to power a hydraulic pump through a hydraulic system, which supplies a generator.

The tapered channel system, or the TAPCHAN, is developed by Norwave AS of Norway. It applies the working principle of a traditional hydroelectric power plant. The seawater is tapered into the reservoir constructed on a cliff and then flows back to the sea through a low-head hydroelectric generator to generate electricity.

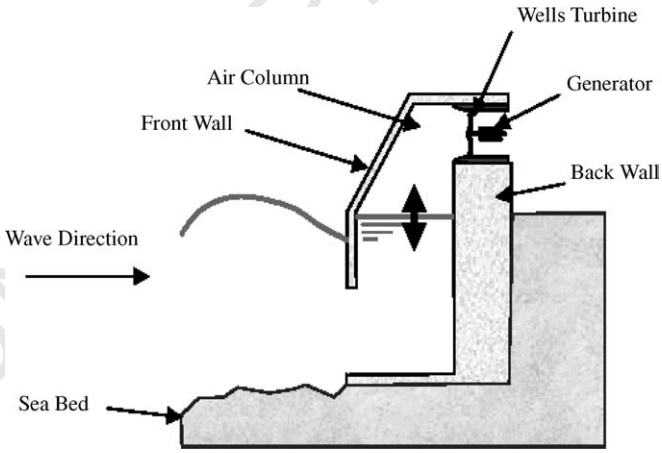

Fig. 1. Working principle of OWC.

UNCORRECTED PROOF

2.2. Nearshore devices

Nearshore devices are in between the shoreline devices and offshore devices. Nearshore devices are characterized by being used to extract the power directly from the breaker zone and the waters immediately beyond the breaker zone. Again, several approaches have been proposed.

The ocean swell powered renewable energy (OSPREY) is designed to operate in 15 m of water within 1 km of the shore, generating up to 2 MW of power for coastal consumers [2]. The Mighty Whale is a floating OWC based device developed by JAMSTEC. A 120 kW prototype with three OWC's in a row has been operating since 1998 in water depths of 40 m, 1.5 km off Nansei Town in Japan. The wind and ocean swell power (WOSP), is an integrated near shore wave and wind powered station. It is designed to operate much the same as the OSPREY device, generating 3.5 MW of power, and offers major advances in accessing multiple offshore renewable energy resources [2]. Another example of a nearshore device is the Pelamis developed by Ocean Power Delivery in Edinburgh, Scotland [4]. This is a semi-submerged, articulated structure composed of cylindrical sections linked by hinged joints. As the waves peak and trough, the sections of the Pelamis act as a pump and move hydraulic fluid through hydro-turbine generators. The power generated from each segment runs to an underwater substation and then to land via a submersible electric cable. A 750 kW prototype of the OPD Pelamis was tested in August 2004 off the coast of Orkney, Scotland.

2.3. Offshore devices

Offshore devices, such as the proposed buoy generator, are the farthest out to sea; they extend beyond the breaker lines and utilize the high energy densities and higher power wave profiles available in the deep-water (>40 m) waves and surges. In order to extract the maximum amount of energy from the waves, the devices need to be at or near the surface. This makes it a requirement to have flexible moorings. In addition, for utility grid support applications, submersible electrical cables are needed to transmit the generated power onto land where they can be interconnected to the grid. The devices can be placed in such a way that they have little visible impact (>2 miles offshore) and can actually provide homes for many aquatic creatures, similar to an artificial reef.

The AquaBuoy is one such offshore buoy system [5]. The technology was originally patented in Sweden, and is now being promoted by the AquaEnergy Group of Mercer Island, Washington. The up and down motions of ocean waves cause pressure changes which draws seawater into a hose pump. This pressurized water is expelled into a collecting line leading to a turbine, which generates electricity. The individual sizes of the buoys are designed according to the energy content of the prevailing seas at a particular installation site. The capacity of the plant is scalable by using different numbers of buoys [5]. A similar approach (The PowerBuoy) has been developed by Ocean Power Technology (OPT) in the US [6].

The McCabe Wave Pump (Haydam Ltd) consists of three narrow rectangular steel pontoons, which are hinged together across their beam pointing into the incoming waves [7]. The fore and the aft pontoons move in relation to the central pontoon by pitching about the hinges, and energy is extracted from this limited rotation by linear hydraulic rams mounted between the central and two outer pontoons near the hinges. This energy can be

UNCORRECTED PROOF

used either to provide electricity by driving a hydraulic motor attached to a generator or to produce potable water by supplying pressurized sea water to a reverse osmosis plant.

The Archimedes Wave Swing (Teamwork Technology in the Netherlands) consists of a cylindrical, air filled chamber (the 'floater'), which can move vertically with respect to the cylindrical 'basement' which is fixed to the sea bed [8]. The air within the 10–20 m diameter 'floater' ensures buoyancy. When a wave passes over the top of the device, it alternatively pressurizes and depressurizes the floater, and the buoyancy is changed which causes the floater to move up and down with respect to the basement. This relative motion is then used to produce electricity.

2.4. Comparisons of different technologies

Shoreline devices have the advantages of easier access for installation and maintenance and they do not need deep-water moorings or long underwater electrical cables. However, when a wave travels towards the shoreline, its power is greatly reduced by the friction caused by the rough seabed. This can be partially compensated by sitting the devices at locations of natural energy concentration.

Offshore devices can take advantage of the more powerful wave profiles available in deeper water (>40 m depth). In order to extract the maximum amount of energy from the waves, the devices need to be at or near the surface and so they usually require flexible moorings and submarine electrical cables for power transmission. These features cause critical cost issues in construction and maintenance.

Nearshore devices exhibit compromises between shoreline and offshore devices, e.g. when there are environmental objections to shoreline devices, near shore devices can provide an alternative solution.

3. Proposed permanent magnet linear generator buoy

3.1. Overview

The objectives and scope of this paper are to describe the research, design, construction and prototype testing process of a novel direct drive permanent magnet linear generator buoy. The design criteria priorities (survivability, reliability and maintainability) drove the decision to use a linear electric generator because such a device experiences low mechanical wear due to low relative speeds in the bearings and bushings. Additionally, a linear generator simplifies the overall mechanical design of the drive components by eliminating the complex and inefficient process of converting the linear thrust of the waves to rotational torque by hydraulic means.

The proposed buoy employs the vertical motion of ocean waves to power a linear generator. The generator consists of a permanent magnet field system (mounted on the central translator shaft) and an armature, in which the power is generated (mounted on the buoy). The translator shaft is anchored to the sea floor, and the buoy/floater moves armature coils relative to the permanent magnet translator to induce voltages. The translator shaft consists of an assembly of high permeability steel pole tip pieces

UNCORRECTED PROOF

(needed for the transfer and direction of flux) and high field strength neodymium-iron-boron magnets (the magnet poles are placed in opposition to effectively concentrate the available flux). The concentrated, two-phase armature coils are wrapped with a spiral of thin electrical lamination steel to provide the flux return path through the generator.

In this design the armature was placed on the 'floater' component of the buoy and moves relative to the translator, although the opposite design, an external magnet topology, can also be employed. The chosen design was found to simplify the construction of the axially magnetized machine, and also reduced the diameter/size of the magnets and pole pieces. Consequently the overall dimensions of the machine were reduced. For larger machines, as well as radially magnetized machines, the possibility of using an external magnet topology could be investigated.

3.2. Power take-off/electrical configuration

An overview of the energy conversion and conditioning process is represented in Fig. 2. The design of the power take off (PTO) from the generator to the load allows for future expansion. The preliminary PTO design consists of a full wave bridge rectifier at the output of each phase of the generator. The two rectifiers are then wired in series to provide the total terminal outputs. A capacitor bank is added to provide a consistent smoothed, rectified voltage.

3.3. Mechanical structure of the buoy/generator

3.3.1. Buoy

The buoy is a cylindrical spar type, fabricated from a 0.4 m diameter, 1.2 m long PVC pipe shown in Fig. 3. The horizontal cross-like struts that attach the armature to the buoy are made from delrin material and are bolted to the buoy structure, with seals. The buoy is equipped with

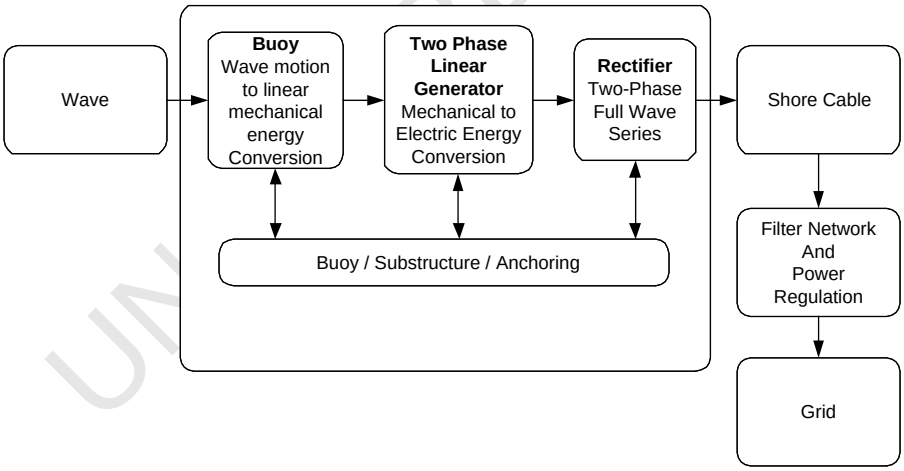

Fig. 2. System block diagram.

UNCORRECTED PROOF

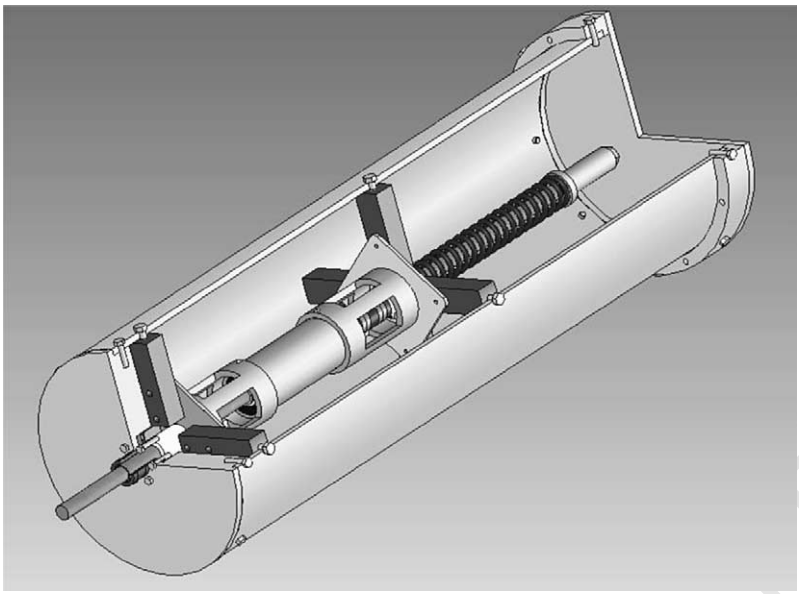

Fig. 3. Buoy mechanical configuration.

flange style end caps and a compression spring located at the top of the generator. The spring can be preloaded using a threaded adjustment device placed at the top of the translator shaft and locked with a lock nut; thus enabling the buoy return stroke to be optimized.

Fig. 3 also shows the solid model design of the buoy and internal structural components. The simple buoy design is a deliberate effort aimed at using non-corrosive materials and avoiding too many moving components that would otherwise compromise reliability, and other stringent requirements in an ocean environment.

3.3.2. Translator shaft and armature

The translator is made up of an alternating assembly of 0.010 m thick Neodymium–Iron–Boron (Nd–Fe–B) permanent magnets, interspersed with soft iron pole pieces mounted on a threaded aluminium shaft as shown in Fig. 4. The magnets are stacked in pairs such that opposing magnetomotive forces (mmfs) drive the flux through the soft iron. Thus, the thickness of each magnet pair and the iron poles are both 0.020 m. This results in a pole pitch of 0.040 m and the total length of the system is 0.320 m. As the armature system moves with respect to the permanent magnet system on the central shaft, its coils experience a change in flux linkage and emf is generated.

The two-phase armature consists of a thin walled tube wrapped with 97 turns of copper magnet wire forming eight individual coil sections. The coil section spacing of 0.020 m, combined with a pole spacing of 0.040 m results in 90 degrees of phase shift between adjacent coil sections. The coil sections were insulated from each other by means of mica spacers placed between each coil. To provide a return path for the flux, the armature coils are wrapped with thin lamination steel. The steel core is then encased in a cylindrical aluminium

UNCORRECTED PROOF

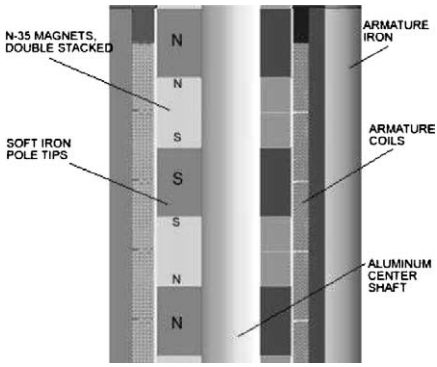

Fig. 4. Partial cross section of generator magnetic circuit.

shell for mechanical support. The parametric dimensions of the generator are given in Table 1 and shown in Fig. 5. The rating of the generator is given in the Appendix A.

4. Simulation results

Analytical calculation and dynamic simulation of the buoy and power take-off was performed using Matlab and Simulink. The equivalent circuit for the PM generator for both electrical and magnetic circuits are shown in Fig. 6.

The voltages of the stator phases A and B can be obtained from the following equations,

$$v_j = -r_j i_j + \frac{\mathrm{d}\lambda_j}{\mathrm{d}t} \quad j = 1, 2 \tag{1}$$

$$\lambda_j = \sum_{k=1}^{2} L_{jk} i_k + \lambda_{jf}$$

where

r phase resistance
i_j current of jth phase

Table 1
Parametric dimensions of generator

Total thickness of magnet pair	0.02 m
Magnet external diameter	0.045 m
Magnet internal diameter	0.020 m
Steel spacer thickness	0.02 m
Total translator length	0.32 m
Number of stator poles	4
Height of coil section	0.02 m
Radial width of coil section	0.006 m
Air gap clearance	0.0006 m

UNCORRECTED PROOF

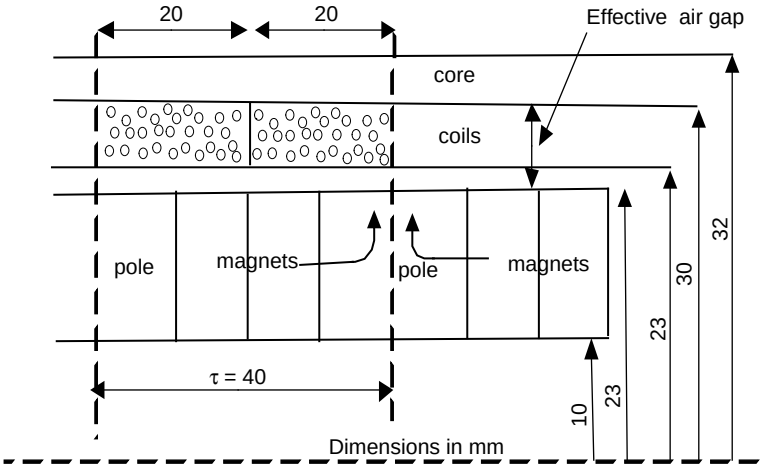

Fig. 5. Dimensions of magnetic circuit.

λ_{jf} flux linkage in phase j due to the magnet
L_{jk}, $j,k=1,2$ are self ($j=$k) and mutual ($j\neq$k) inductances.

The self and mutual inductances in general are position dependent and their analysis is complex [16]. The flux linkage due to the permanent magnet depends on the pole pitch and the displacement. The maximum flux linkage occurs when the axis of the coil is aligned with that of the soft iron pole. Under these conditions we have maximum emf at

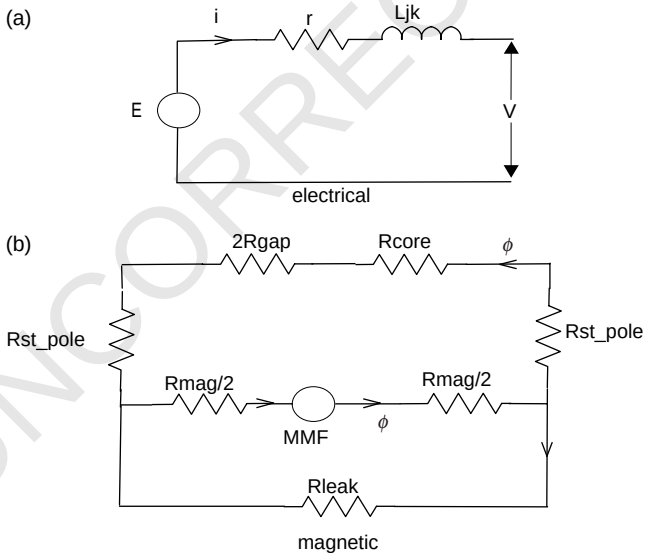

Fig. 6. Equivalent circuits.

UNCORRECTED PROOF

peak linear speed. With the pole pitch fixed at 40 mm, the flux linking a coil is dependent on the relative motion between the translator shaft and stator.

The emf of a phase is given by

$$E_j = \frac{\mathrm{d}\lambda_{jf}}{\mathrm{d}t} = \frac{\mathrm{d}\lambda_{jf}}{\mathrm{d}z}\frac{\mathrm{d}z}{\mathrm{d}t} \tag{2}$$

where

$$\lambda 1\mathrm{f} = \mathrm{N}\phi 1 = \mathrm{N}\phi \mathrm{c\hat{o}s}((\pi/\tau)\mathrm{z})$$

flux linkage of phase A (note phase B is shifted by 90°)

z displacement of the translator relative to the stator
τ pole pitch of the generator
N number of turns in phase
$\hat{\phi}$ peak flux

Expanding Eqs. (1) and (2) and simplifying, we have for example for phase A:

$$v_1 = -r_1 i_1 + L_{11}\frac{\mathrm{d}i_1}{\mathrm{d}t} + L_{12}\frac{\mathrm{d}i_2}{\mathrm{d}t} + \frac{\mathrm{d}\lambda_{1f}}{\mathrm{d}t} \tag{3}$$

$$E_1 = \frac{\mathrm{d}\lambda_{jf}}{\mathrm{d}t} = -N\hat{\phi}\frac{\pi}{\tau}\sin\left(\frac{\pi}{\tau}z\right)\frac{\mathrm{d}z}{\mathrm{d}t} \tag{4}$$

Hence the current of phase A can be obtained from Eq. (5):

$$\frac{\mathrm{d}i_1}{\mathrm{d}t} = \frac{1}{L_{11}}\left(v_1 + r_1 i_1 - L_{12}\frac{\mathrm{d}i_2}{\mathrm{d}t} - E_1\right) \tag{5}$$

The above equations were programmed into Matlab/Simulink to compute the value for the current of each phase. The peak flux for the analytical calculations was obtained from the simple equivalent circuit of the magnetic circuit shown in Fig. 6, where the reluctances can easily be calculated from the dimensions in Fig. 5. The inductances were obtained from finite element analysis, discussed subsequently.

A typical emf at no-load obtained by simulation is shown in Fig. 7. This is superimposed with the buoy speed of motion (peak speed = 0.5 m/s, period = 3 s) and shows the virtually zero voltage at zero speed as expected. The rectified output from the simulation is given on the same figure. For comparison a typical oscilloscope capture of the output of the generator when it is excited by sinusoidally varying speed from a reciprocating device is shown in Fig. 8, where the traces from top to bottom on the scope capture, are the rectified voltage, current, output power and input power, respectively.

The simulation of the generator buoy system was carried out by considering all the forces on the oscillating structure including the hydrodynamic forces. In a simplified form, the single degree of freedom (heave) motion of the buoy can be represented by the following equation:

$$m_{\mathrm{v}}\ddot{z} + b\dot{z} + cz + f = F_0\cos(\omega t + \sigma) \tag{6}$$

where

UNCORRECTED PROOF

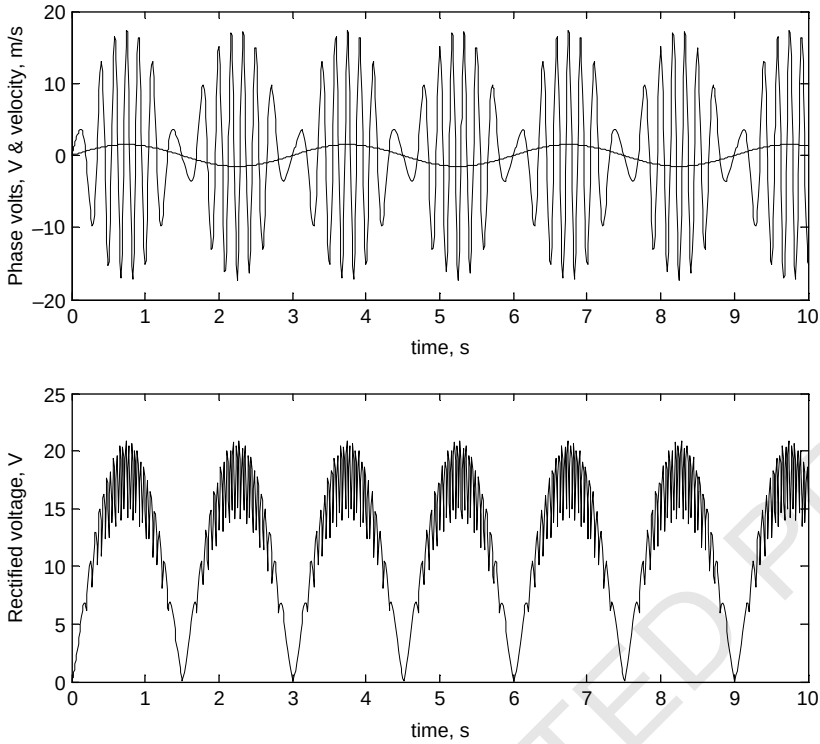

Fig. 7. Idealized generated no-load emf and rectified voltage.

m_v is the virtual mass of the buoy including added mass
b is the hydrodynamic damping
c is the spring constant
f is the thrust from the linear generator

$$F = F_0 \cos(\omega t + \sigma)$$

is the exciting wave force
z buoy vertical displacement

The added mass and hydrodynamic damping are generally, frequency dependent. An expression for the added mass for a cylindrical buoy can be found in [12]. Applying expressions derived in [12], the hydrodynamic damping for the cylinder is given by:

$$b = \frac{\pi^2 \rho g^2}{8\omega_n^3} \bar{A}^2 D \tag{7}$$

where

ρ density of water
$\omega n = \sqrt{c/mv}$ natural frequency of buoy in heave

UNCORRECTED PROOF

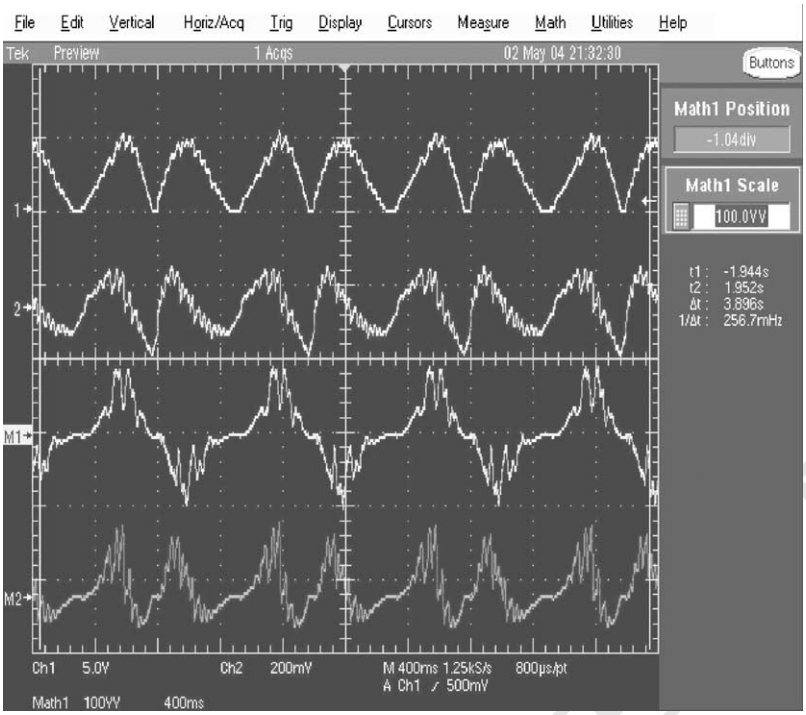

Fig. 8. Typical test results using reciprocating device.

D diameter of buoy
A^- ratio of wave amplitude and amplitude of motion

The total thrust on the coils of the machine is position dependent and can be expressed as

$$f = f_n \cos\left(\frac{\pi z}{\tau}\right) \tag{8}$$

The peak thrust generated can be approximated from the product of the instantaneous values of the no-load voltages and current and divided by the speed. This is given by:

$$f_n = -N\frac{\pi}{\tau}\hat{\phi}\hat{i}\cos\varphi \tag{9}$$

ϕ is the phase angle between the voltage and current

5. Finite element modeling

A 2D finite element (FE) model of the linear generator was implemented, using Maxwell®2D from Ansoft Corporation. The finite element analysis provided results

UNCORRECTED PROOF

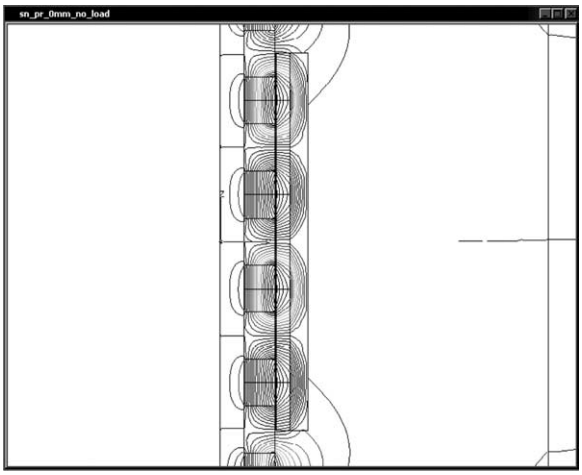

Fig. 9. Flux in the generator.

for the flux linkage and inductances that was used in the analytical computations for determination of current as well as thrust. The FE model also provided a 'sanity check' for some of the analytical calculations. Fig. 9 shows a typical flux plot from the FE analysis of the generator for a given position of the translator. Also shown in Fig. 10 is the magnitude of the magnetic flux density in along an axial line drawn in the air-gap of the machine (near the translator surface) at a given time. Fig. 11 is a comparison of the analytical approximation of the thrust with that obtained from the FE model. The FE results shows the effects of harmonics and the saliency of the translator field that were not considered in the analytical approximations of the thrust.

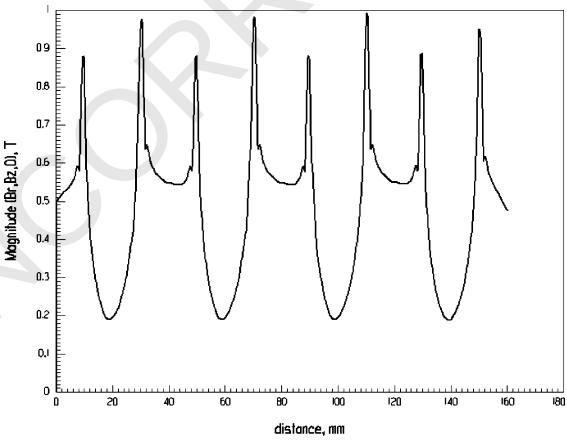

Fig. 10. Magnetic flux density.

UNCORRECTED PROOF

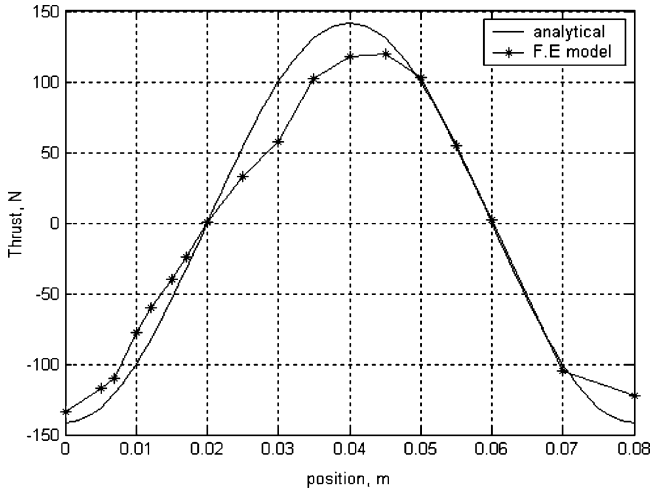

Fig. 11. Thrust as function of position.

6. Preliminary experimental results

6.1. Laboratory tests

The linear generator was tested with a reciprocating device that simulates the motion of waves and subsequently, an actual wave tank test was performed. The reciprocating device is a 5 hp, 1750, 230 V induction motor coupled to a 30:1 gearbox and a crank and lever mechanism (Fig. 12). The motor is fed through a variable frequency drive, thus providing linear speeds in the range of 0–2 m/s. The reciprocating device tests were conducted in the Motor Systems Resource Facility (MSRF) laboratory.

The MSRF is currently the highest power, energy systems laboratory in any university in the nation (750 kVA) with full capabilities to regenerate back onto the utility grid for experimental simulations of the operation of renewables. The MSRF includes comprehensive testbeds up to 300 hp and a 120 kVA fully programmable source (Fig. 13).

Fig. 14 shows typical test results obtained during tests with the reciprocating device, showing, from top down, the unrectified phase voltage, the rectified voltage, current and output power, respectively. The measured performance of the generator under controlled laboratory conditions of adjustable loads is summarized in Figs. 15 and 16. The voltage speed curve in Fig. 15 as expected is linear over the design rated speed of 0.5 m/s. Also in Fig. 16, the highest output power was obtained at the 1.4 Ω load which is close to the source resistance of the generator. Other test results under various load conditions are given in the Appendix A.

6.2. Wave flume tests

Preliminary wave flume testing has also been conducted in the O. H. Hinsdale Wave Research Laboratory (WRL) at OSU, one of the world's largest and best-controlled

UNCORRECTED PROOF

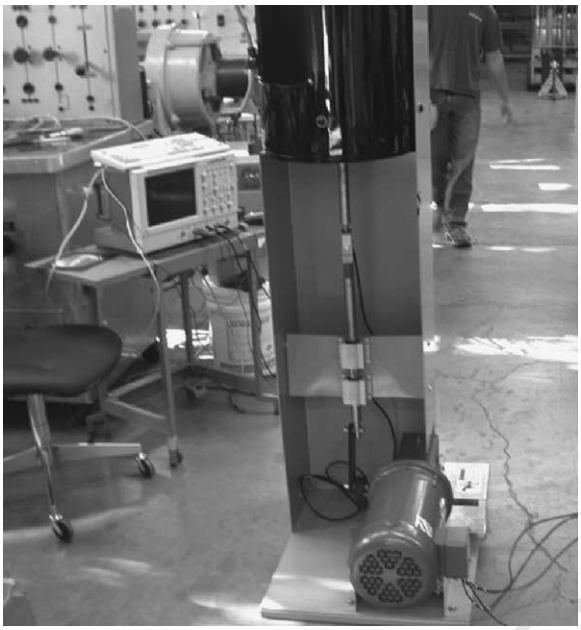

Fig. 12. Reciprocating device and load cell.

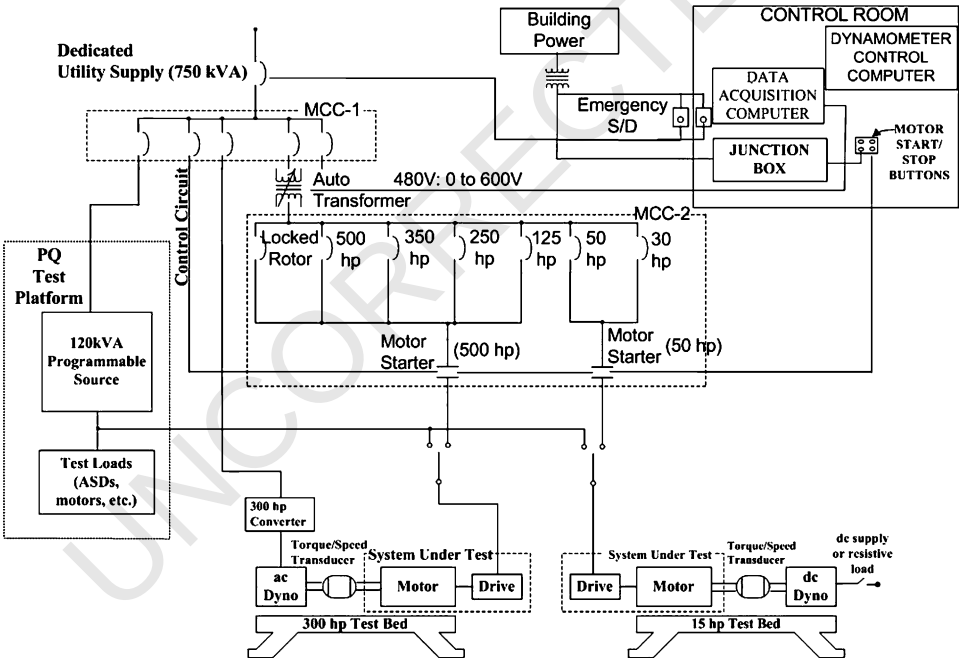

Fig. 13. Schematic representation of OSU's MSRF.

UNCORRECTED PROOF

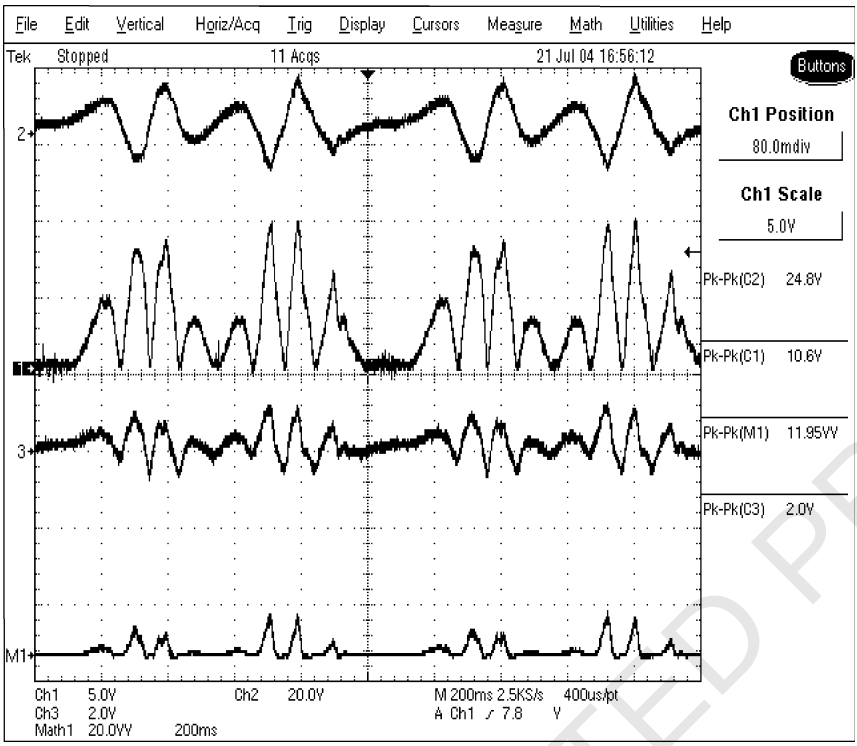

Fig. 14. Typical scope capture showing voltage, current and output power.

systems of wave basins (Fig. 17). The combination of these strategic facilities (MSRF and WRL), as well as the strong team of multidisciplinary researchers, graduate students and undergraduates enhance the contributions OSU is making towards ocean energy development both through innovative technologies as well as integrated systems

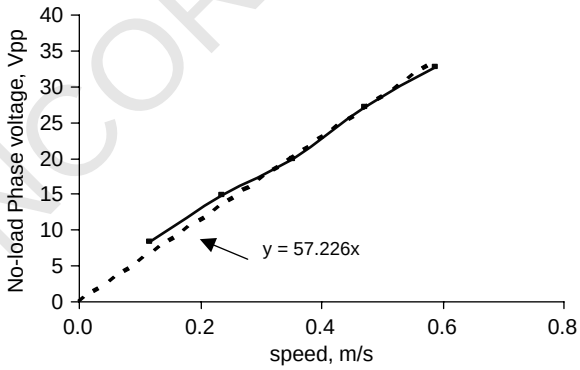

Fig. 15. No-load phase voltage.

UNCORRECTED PROOF

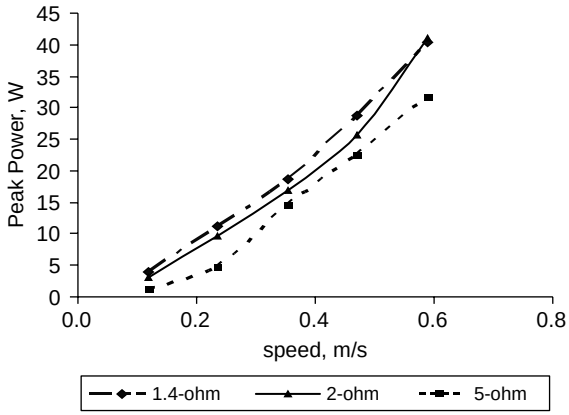

Fig. 16. Peak power under load.

engineering research and testing. The device was tested in regular waves of different heights and wave periods.

Fig. 17 shows no load output voltage of the generator in a 3 ft, 3 s wave. The lower waveform depicts the wave surface elevation. At the initial tests it was evident that the stroke has to be optimized. As shown in the tank test results in Appendix B, the power output obtained from the generator during actual wave flume testing in the WRL was expectedly less than that obtained during the reciprocating device tests in the MSRF. One explanation is that the buoy was not constrained in the heave mode (z-direction) only and therefore energy was dissipated in other modes of oscillation. The reciprocating device test is essentially a single degree of freedom (heave) test while in the wave tank six degrees of freedom are possible and were observed. Other factors are also being investigated (Fig. 18).

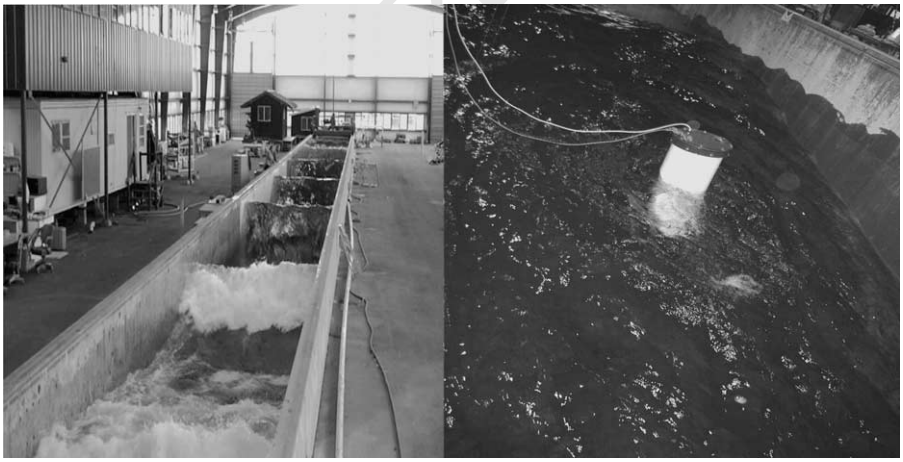

Fig. 17. Prototype testing in the O. H. Hinsdale Wave Research Laboratory.

UNCORRECTED PROOF

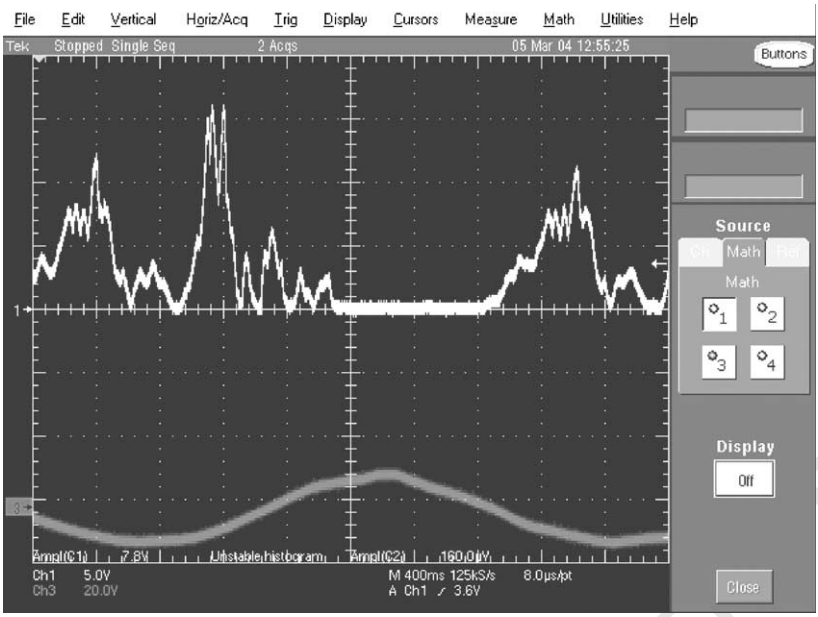

Fig. 18. Typical test result from wave tank.

7. Conclusions

A novel permanent magnet linear generator buoy that utilizes the direct motion of ocean waves to generate electricity has beenl designed, built and tested. The prototype device is a two-phase linear generator capable of generating up to 50 W. Wave tank testing and optimization of the device are currently ongoing, as well as investigations of other direct drive approaches. In addition, finite element modeling, simulations and analytical performance of a linear generator was compared to actual performance in an ocean wave buoy generator application and shows good correlation. This small-scale demonstration device presents a direct drive buoy wave energy collection system as one possible alternative to more mechanically complex hydraulic systems. Additionally, this demonstration device performance in 1.5 m waves indicates satisfactory completion of the project goals of survivability and reliability.

8. Uncited references

[9]. [10]. [11]. [13]. [14]. [15]. [17].

Acknowledgements

The authors wish to acknowledge the National Science Foundation for the funding and support of this research. This material is based upon work supported under Grant No. 0300386.

UNCORRECTED PROOF

Appendix A

Electrical parameters of the generator

Rated voltage	25 V
Rated current	3 A
Rated power output	50 W
Number of phases	2

Appendix B

Wave tank tests

Load (ohm)	Wave height (m)	Wave period (s)	Peak voltage (V)	Peak current (A)	Peak power (W)
5	1.37	3	20	1.4	25
2	1.37	3	16	1.6	18
10	1.37	3	19	1.2	12
5	0.98	3	12	0.6	6
5	1.21	3	10	0.5	5
5	0.66	3	9	0.5	5
2	0.98	3	6	0.7	4
5	0.98	2	10	0.5	3.6
2	0.82	6	2.4	0.1	0.2
10	0.98	3	20	0	0
No load	0.98	3	20	0	0

Appendix C. Solid model of generator

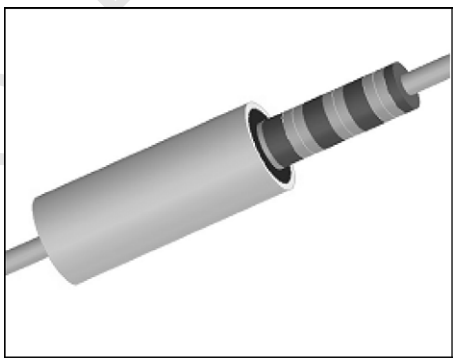

UNCORRECTED PROOF

References

[1] http://www.nrel.gov.
[2] http://www.wavegen.co.uk.
[3] http://www.energetech.com.au.
[4] http://www.oceanpd.com.
[5] http://www.aquaenergygroup.com/.
[6] http://www.oceanpowertechnologies.com/.
[7] http://wave-power.com/.
[8] http://www.waveswing.com/.
[9] ANSI/IEEE Std 1021-1988, IEEE Recommended practice for utility interconnection of small wind energy conversion systems.
[10] http://bigfoot.wes.army.mil/u043.html.
[11] Thorpe TW. A brief review of wave energy—a report produced for the UK department of trade and industry, May 1999.
[12] McCormick ME. Ocean engineering wave mechanics. London: Wiley; 1973.
[13] Falnes J. Ocean waves and oscillating systems. Cambridge: Cambridge University Press; 2002.
[14] Nasar SA, Boldea I. Linear electric motors. Englewood Cliffs, NJ: Prentice Hall; 1987.
[15] Fitzgerald AE, Kingsley C, Umans SD. Electric machinery. New DelhiTavistock: McGraw Hill; 1990.
[16] Wang J, Jewell GW, Howe D. A general framework for the analysis and design of tubular linear permanent magnet machines. IEEE Trans Magn 1999;35(3).
[17] Ansoft Corporation, Maxwell®2D.

UNCORRECTED PROOF